Supplementary Information

Effects of Hydration Water on Bioresponsiveness of Polymer Interfaces Revealed by Analysis of Linear and Cyclic Polymer–Grafted Substrates

Shin-Nosuke Nishimura[a,d‡], Naoya Kurahashi[b,c‡], Shohei Shiomoto[a‡§], Yoshihisa Harada[c,e*], and Masaru Tanaka[a*]

[a] *Institute for Materials Chemistry and Engineering, Kyushu University, 744 Motooka, Nishi-ku, Fukuoka 819-0395, Japan*

[b] *Department of Materials Molecular Science, Institute for Molecular Science, 38 Nishigonaka, Myodaijicho, Okazaki, Aichi 444-8585, Japan*

[c] *Institute for Solid State Physics, The University of Tokyo, 5-1-5 Kashiwanoha, Kashiwa, Chiba 277-8581, Japan*

[d] *Department of Molecular Chemistry and Biochemistry, Faculty of Science and Engineering, Doshisha University, 1-3 Tatara Miyakodani, Kyotanabe, Kyoto 610-0394, Japan*

[f] *Synchrotron Radiation Collaborative Research Organization, The University of Tokyo, 468-1 Aoba, Aramaki, Aoba-ku, Sendai, Miyagi 980-8572, Japan*

‡S.N., N.K., and S.S. contributed equally to this paper.

§Present address: *Department of Materials Science and Technology, Faculty of Advanced Engineering, Tokyo University of Science, 6-3-1 Niijyuku, Katsushika, Tokyo 125-8585, Japan*

*Email: masaru_tanaka@ms.ifoc.kyushu-u.ac.jp (M.T.), harada@issp.u-tokyo.ac.jp (Y.H.)

Table of Contents

1 DETAILED EXPERIMENTAL PROCEDURES

1.1 Human Platelet Adhesion Experiments

Human whole blood was centrifuged at 400 *g* for 5 min to collect platelet-rich plasma (PRP), and the residue was centrifuged at 2500 *g* for 10 min to collect platelet-poor plasma (PPP). The concentration of platelets in the PRP solution was adjusted to 3.0×10^7 cells/cm^3 by mixing with the PPP solution. The desired polymer-grafted substrate was soaked in PBS(–) for 1 h, incubated in the platelet solution at 37 °C for 1 h, rinsed with PBS(–), incubated in 1% glutaraldehyde in PBS(–) at 37 °C for 2 h to fix the adhered platelets, sequentially washed with PBS(–) and pure water, and naturally dried for one day at room temperature. The number of adhered platelets was determined by scanning electron microscopy.

1.2 Cell Adhesion Experiments

The polymer-grafted substrate (ϕ = 14 mm) was placed into a 24-well polystyrene plate (Iwaki, AGC Techno Glass Co., Ltd., Japan), soaked in PBS(–), sterilized using ultraviolet light (254 nm) for 30 min, and seeded with cells (1.0×10^4 cells/cm^2) at 37 °C for 6 h (5% CO_2) in a serum-containing medium. The adhered-cell morphology was observed using a phase-contrast microscope (CKX53; Olympus Co., Japan). The number of adhered cells was determined using the WST-8 assay as follows. After culturing, the medium was removed, and 450 μL of fresh Dulbecco's Modified Eagle Medium without phenol red was added to the cell-adhered samples. The sample was treated with 50 μL of the solution used for the WST-8 assay, i.e., PBS(–) containing WST-8 (5 mM) and 1-methoxy PMS (200 μM), and incubated at 37 °C for 1 h. The supernatant (200 μL) was poured into a 96-well polystyrene plate and subjected to absorbance measurement at 450 nm. The number of adhered cells was determined using a calibration curve.

1.3 Atomic Force Microscopy (AFM) Observations

AFM observation was performed in PeakForce Tapping® (PFT)-mode using a cantilever (MSNL-F, Bruker, spring constant (k) = 0.6 N/m, resonance frequency (f) = 125 kHz (in air)). Measurements were performed at a fixed peak force frequency of 1 kHz and peak force of 1 nN. For frequency modulation (FM)-AFM observations, a cantilever with a square pyramidal tip (PPP-NCHAuD, NanoWorld AG, k = 24 N/m, f = 330 kHz (in air)) was used at a resonance frequency of 140 kHz in water and force limit of 1 V (corresponding to a frequency shift of ~ 200 Hz). The change in the resonance frequency was recorded in the xz (surface-normal) direction at a scan rate of 10 Hz for the first scan (z-direction). The peak-to-peak amplitude of the cantilever oscillation remained constant at ~3.0 nm. The same cantilever was used for both *gl*-PMEA and *gc*-PMEA. Trace images were obtained at different points to ensure the reproducibility of the FM- and PFT-AFM measurements.

1.4 Swelling Behavior of Grafted PMEAs in Ionic Aqueous Solution

FM-AFM observations of *gl*-PMEA and *gc*-PMEA were performed in an ionic aqueous solution under the same AFM control conditions as those used in pure water. After the observations in pure water, the pure water in the petri dishes, which were attached the sample substrates, were replaced with phosphate-buffered saline (PBS) not containing calcium and magnesium ions.

As shown in the FM-AFM images (Figure S3) acquired perpendicular to the substrates showed repulsive layers above the substrates, indicating the swelling layers of the *gl*-PMEA and *gc*-PMEA in PBS. The measured thicknesses of the swelling layers were approximately 13 nm and 16 nm for the *gl*-PMEA and *gc*-PMEA, respectively. Both of PMEA-grafted layers were shrunk in PBS

compared to those in pure water. The composition of PBS includes NaCl, KCl, Na_2HPO_4, KH_2PO_4. The salts caused dehydration of PMEA and resulted in the shrinking of *gl*-PMEA and *gc*-PMEA, as evidenced by equilibrium water contents of the respective bulk polymers is lower in PBS compared to pure water (ref. 56 in the main manuscript). Although the difference in the swelling thicknesses between the linear and cyclic types in PBS has diminished comparing the result in pure water, the *gc*-PMEA exhibited a thicker swelling thickness than the *gl*-PMEA, even in suffering the salts effect. As mentioned earlier, in the presence of salt cells showed different biological responses at the interface of PMEA with different topologies. Even when the PMEA were shrunk, the different swelling behavior of the chains appears to influence the biological response.

1.5 Quartz Crystal Microbalance (QCM) Measurements

Mirror-finished gold-sputtered QCM substrates (QA-A9M-AU(M), Seiko EG&G Co., Ltd.; fundamental resonance frequency (F_F) = 8.9 MHz) were rinsed with ethanol and treated with an ultraviolet/ozone cleaner (UV253E, Filgen) for 30 min. The substrates were mounted on polyvinyl chloride well-type cells (QA-A9M-AU(M), Seiko EG&G Co., Ltd.) and connected to the QCM system (QCM922A, Seiko EG&G Co., Ltd.). The resonance frequencies of the bare QCM substrates in air ($F_{bare,air}$) were recorded at 23 °C (all QCM measurements were conducted at the same temperature). The corresponding resonance frequencies in water ($F_{bare,water}$) were measured by adding water (200 μL) to the wells of the QCM cells. Subsequently, the added water was removed, and the substrates were dried in low-humidity air (relative humidity < 10%) at room temperature (24 °C). The substrate surfaces were exposed to a methanolic solution of linear PMEA (1 μM, 200 μL) for 20 min or cyclic PMEA (1 μM, 200 μL) for 60 min to obtain the *gl*-PMEA and *gc*-PMEA surfaces, respectively. The substrates were washed five times by replacing the solution

in the wells with methanol and dried in low-humidity air at room temperature for 12 h. The resonance frequencies ($F_{\text{grafted,air}}$) of the polymer-grafted substrates in air were measured and used to determine frequency changes due to polymer grafting ($\Delta F_{\text{grafted,air}}$) as $\Delta F_{\text{grafted,air}} = F_{\text{grafted,air}} - F_{\text{bare,air}}$. These frequency changes were translated into mass changes ($\Delta m_{\text{grafted}}$) corresponding to the mass of the grafted polymer using a method based on the Sauerbrey equation.[1]

$$\Delta m_{grafted} = C\Delta F_{grafted,\ air}, \tag{S1}$$

where C is a collection of constants, namely the area of the gold surface (A = 0.196 cm^2), density of quartz (ρ_q = 2.65 g/cm^3), and shear modulus of quartz (μ_q = 2.95 × 10^{11} g/(cm s^2)).

$$C = -\frac{A\sqrt{\rho_q \mu_q}}{2{F_F}^2}. \tag{S2}$$

The grafting density of polymer chains σ (chains/nm^2) was obtained as

$$\sigma = \frac{\Delta m_{grafted} N_A}{M_n A}, \tag{S3}$$

where N_A is Avogadro's number, and M_n is the number-average molecular weight of the polymer (linear PMEA: 38,000; cyclic PMEA: 75,900). The polymer-grafted substrates were placed in contact with water, and the resonance frequencies ($F_{\text{grafted,water}}$) were measured and used to calculate the frequency change as $\Delta F_{\text{grafted,water}} = F_{\text{grafted,water}} - F_{\text{bare,water}}$ (ref. 61 in the main manuscript).

The observed $\Delta F_{\text{grafted,water}}$ and $\Delta F_{\text{grafted,air}}$ for each substrate are presented in Table S2. The $\Delta F_{\text{grafted,air}}$ was converted to σ using Equations S1 and S3. The σ of both *gl*-PMEA and *gc*-PMEA (0.1 and 0.05 chains/nm^2, respectively) were confirmed to match the intended design. These substrates were utilized for atomic force microscopy (AFM) observations. For cell adhesion studies and X-ray emission spectroscopy (XES), PMEA was grafted onto an additional gold-deposited substrate using the same preparation conditions to achieve the same σ.

The $\Delta F_{grafted,water}$ was greater than $\Delta F_{grafted,air}$ for both *gl*-PMEA and *gc*-PMEA. The ratio of hydrated mass to dry mass ($\Delta F_{grafted,water}/\Delta F_{grafted,air}$) was 1.50 ± 0.13 for *gl*-PMEA and 1.57 ± 0.05 for *gc*-PMEA. ΔF in water is determined by the balance of two factors (ref. 62 in the main manuscript): the first is the friction resulting from the interaction between the molecules immobilized to the substrate and the surrounding hydration water, which increases the apparent mass in water. The second factor is energy dissipation resulting from the viscoelasticity of the immobilized molecules, which reduces the apparent mass in water. For both topologies of grafted PMEA, $\Delta F_{grafted,water}/\Delta F_{grafted,air}$ was greater than 1, indicating that the apparent masses were increased by the hydration. However, since $\Delta F_{grafted,water}/\Delta F_{grafted,air}$ includes the contribution of the molecular viscoelasticity, which gives an error to the precise amount of hydration. The viscoelasticity of a molecule is influenced by its conformation including whether the molecule is elongated and softened in water. For instance, previous studies have reported that long and flexible molecules, such as sugar chains and deoxyribonucleic acid, can influence significantly (ref. 61 in the main manuscript). The viscoelastic properties of *gl*- and *gc*-PMEA are anticipated to differ because the grafted PMEAs existed in distinct chain elongation states in aqueous solution, as observed by the frequency modulation atomic force microscopy (FM-AFM). Molecular-scale analysis of hydration was performed using X-ray emission spectroscopy (XES).

1.6 X-ray Emission Spectroscopy (XES) Measurements

The XES profiles of water at the polymer interface were visually classified into three types (Figure S4). Assuming that each spectrum consists of three or four peaks, multipeak fitting was performed using the fitting functions (symmetric Gaussians, asymmetric Gaussians, and Lorentzians) and initial parameters listed in Table S3.

$$I(E) = \frac{A}{\sqrt{2\pi\sigma^2}} e^{-\frac{(E-\mu)^2}{2\sigma^2}}, \quad \text{(S5)}$$

$$I(E) = \frac{A}{\sqrt{2\pi\{a(E-\mu)+\sigma\}^2}} e^{-\frac{(E-\mu)^2}{2\{a(E-\mu)+\sigma\}^2}}, \quad \text{(S6)}$$

$$I(E) = \frac{A}{\pi} \frac{\gamma}{(E-\mu)^2+\gamma^2}, \quad \text{(S7)}$$

where A is the peak area, σ is the standard deviation in Gaussians (eV), μ is the peak center (eV), a is the asymmetry parameter (eV), and γ is the half-width at half-maximum in the Lorentzian (eV).

The group with the lowest water content exhibited a spectrum similar to that of water vapor (Figure S5). In this case, three peaks were used for fitting. Peaks 1, 2, and 4 in Figure S4A were identified as $1b_2$, $3a_1$, and $1b_1$, respectively, and fitted to asymmetric Gaussians, symmetric Gaussians, and Lorentzians. With increasing water content, a broad peak around 525.9 eV appeared in the water spectrum (Figure S4B). Peaks 1, 2, and 4 were fitted as shown in Figure S3A. The newly appeared peak (Peak 3) was fitted to a Gaussian in view of the absence of theoretical support for the possibility of $1b_1$ splitting. As the water content increased further, the spectral shape became indistinguishable from that of bulk water (Figure S4C), Peaks 3 and 4 disappeared, and Peaks 3' and 3" (considered to be $1b_1$' and $1b_1$", respectively, split from $1b_1$) appeared instead. All peaks could be fitted to a symmetric Gaussian function.

Given that we performed K-edge nonresonant XES measurements of oxygen, we considered the nonresonant XES process to discuss peak shapes. The most stable structure of the water molecule, i.e., the initial state of XES, is $^1A_1$, with the removal of the $1a_1$ (oxygen 1s) electron producing intermediate state $^2A_1$ ($1a_1^{-1}$). This state relaxes to one of the dipole-allowed final states

($^2B_2$ ($1b_2^{-1}$), $^2A_1$ ($3a_1^{-1}$), or $^2B_1$ ($1b_1^{-1}$)) upon the emission of soft X-rays. In the case of significant differences between the nuclear equilibrium points of the initial and intermediate states and those of the intermediate and final states, that is, if the shapes of the corresponding potential energy surfaces are significantly different, the XES profile exhibits a complex structure with multiple vibrational progressions. This behavior is well known from photoelectron spectroscopy (Figure S4). The nuclear equilibrium points of the initial ($^1A_1$) and intermediate ($^2A_1$) states are believed to be nearly identical, which is reasonable because the 1s electrons of oxygen are not involved in the binding of water molecules. As the nuclear equilibrium point of $^2B_1$ ($1b_1^{-1}$) is considered to be close to that of $^2A_1$ (or $^1A_1$), the $1b_1$ transition in the nonresonant XES was observed as a sharp single peak. The peak shape was described by a Lorentzian because of the windowless geometry of the spectrometer. However, the nuclear equilibrium points of $^2A_1$ ($3a_1^{-1}$) and $^2B_2$ ($1b_2^{-1}$) are different from those of the intermediate (or initial) state; therefore, the XES peak had a complicated shape with numerous vibrational progressions. The XES peak was broad because it was observed as an envelope with the natural width superimposed on the vibrational progressions. Therefore, a theoretical explanation of the $3a_1$ and $1b_2$ peaks in nonresonant XES profiles requires at least the calculation of the potential energy surfaces of the intermediate and final states and the time evolution of the electron packets. Hence, the spectral shape of adsorbed water at the solid–liquid interface is difficult to predict, as in the present study. Given that the present work aimed to qualitatively consider the water content dependence of XES peaks, the $1b_2$ and $3a_1$ peaks were characterized assuming a symmetric or asymmetric Gaussian envelope.

2 Supplementary Figures

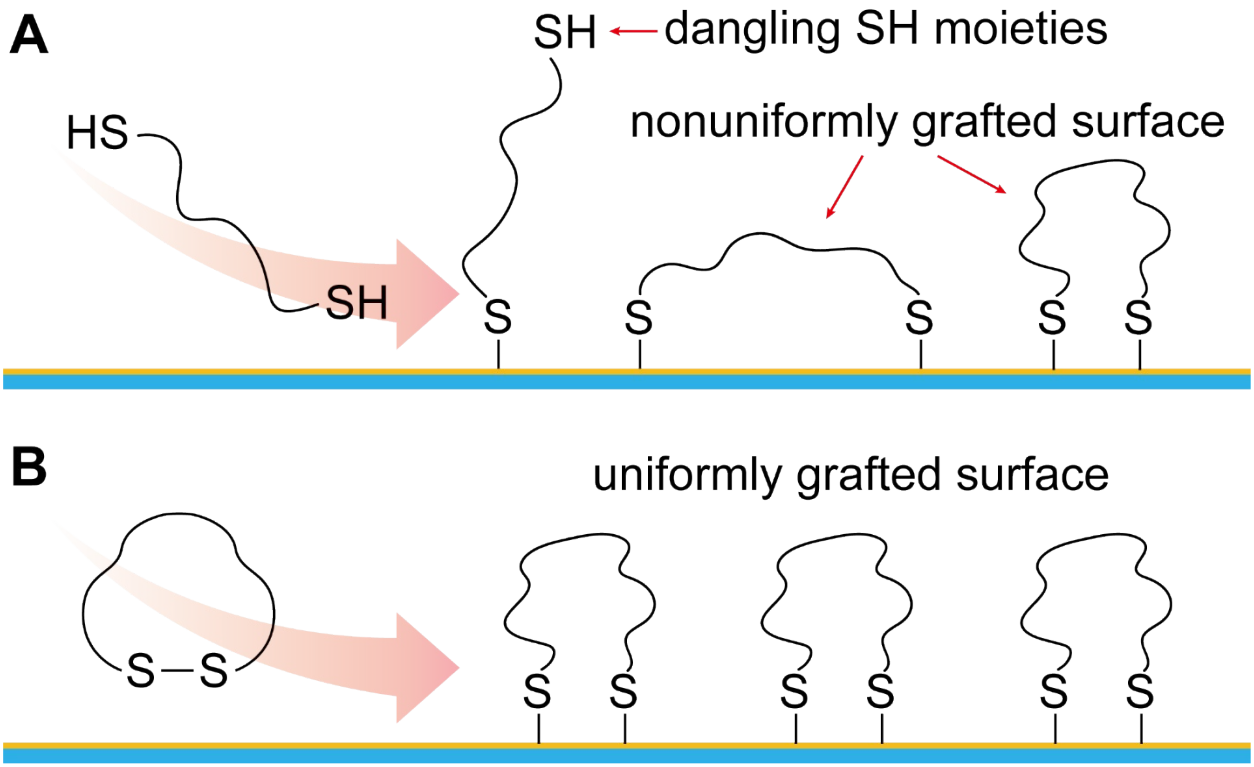

Figure S1. Schematic preparation of polymer-grafted surfaces using (A) a dithiol-type polymer (*l*-PMEA) and (B) a precyclized polymer containing disulfide bonds (c-PMEA).

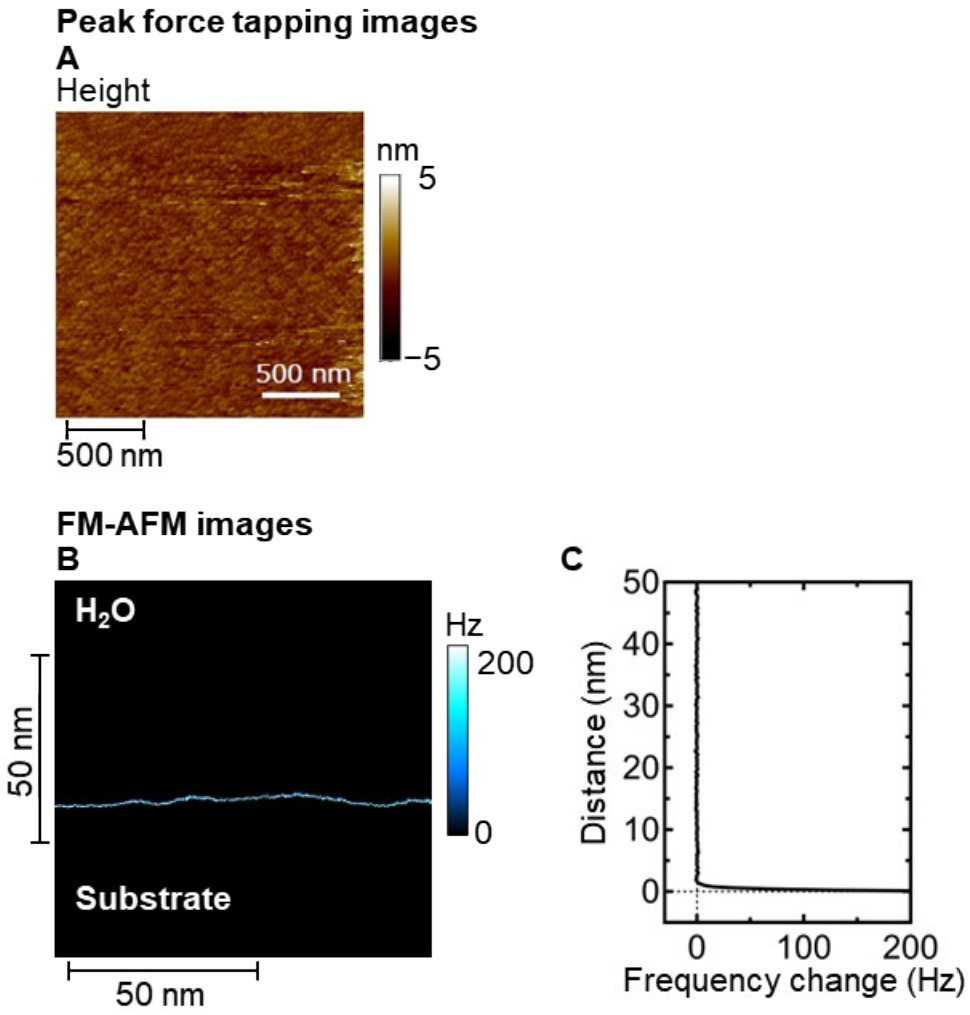

Figure S2. (A) Height image of a bare gold-coated QCM substrate obtained by PeakForce Tapping® (PFT)-mode atomic force microscopy (AFM) in water; (B) *xz*-directional frequency modulation (FM)-AFM images of the gold substrate and (C) frequency change–*z*-distance curves recorded in water.

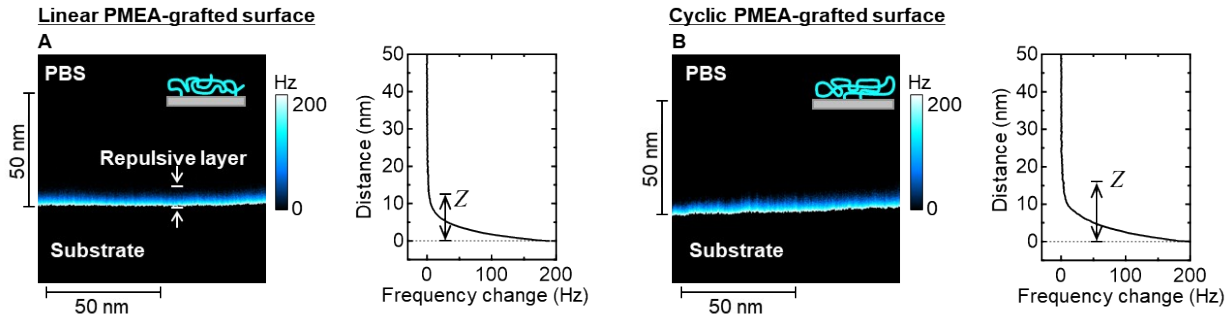

Figure S3. *xz*-directional frequency modulation (FM)-AFM images (scan area = 100 nm × 50 nm) and *z*-directional frequency curves of (A) *gl*-PMEA and (B) *gc*-PMEA interfaces in PBS.

`

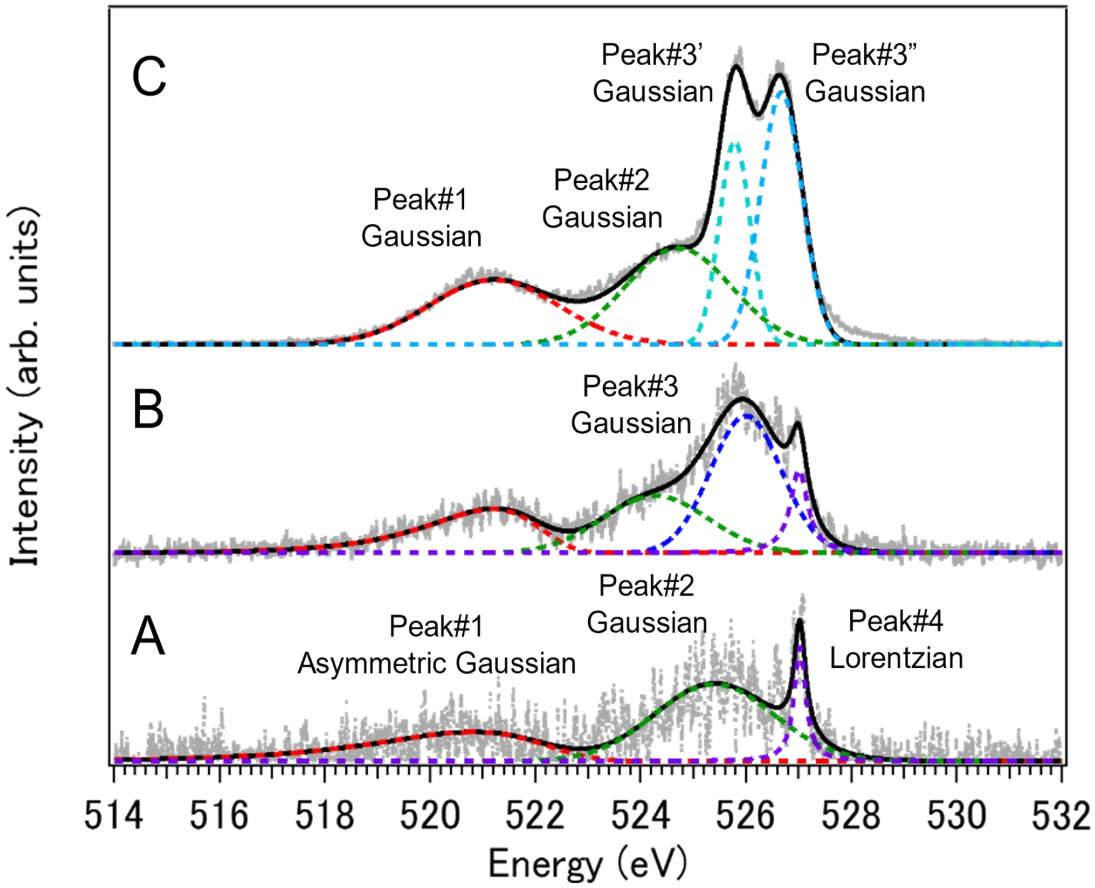

Figure S4. Representative X-ray emission spectra of *gl*-PMEA interfacial water. The experimental data are presented as gray dots, with solid black lines corresponding to multipeak fitting envelopes and colored dashed lines presenting the results of peak deconvolution. (A) At WC = 25.0%, the spectrum consists of Peaks 1, 2, and 4 with asymmetric Gaussian, symmetric Gaussian, and Lorentzian envelopes, respectively. (B) At WC = 61.8%, the spectrum consists of Peaks 1, 2, 3, and 4, with Peak 3 fitted by a symmetric Gaussian; (C) At WC = 94.7%, the spectrum is similar to that of bulk water and features Peaks 1, 2, 3', and 3" that can be fitted by a Gaussian.

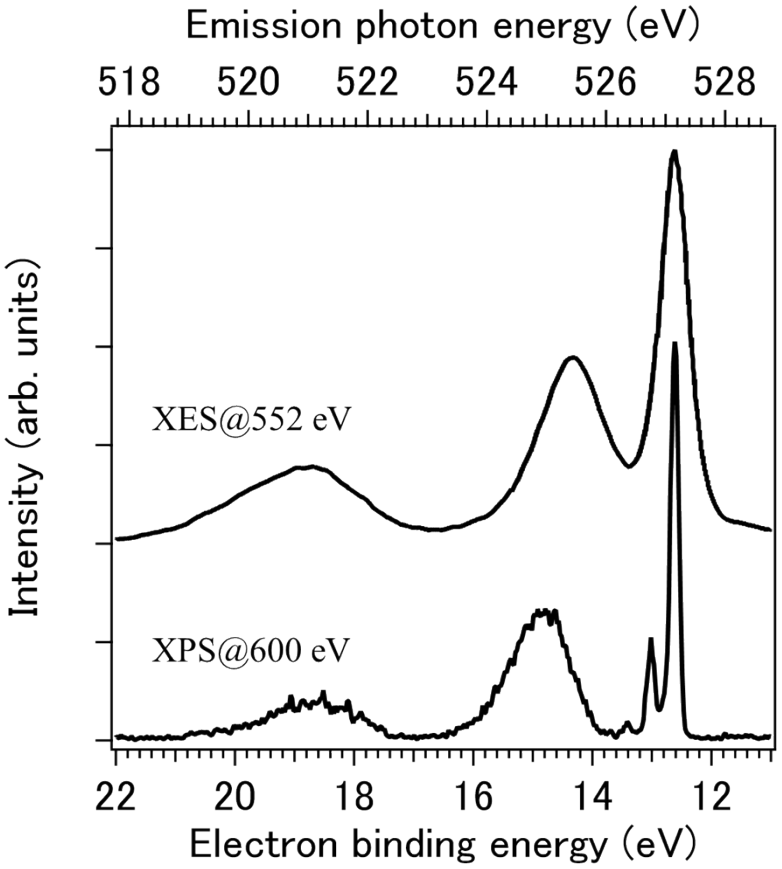

Figure S5. Soft X-ray photoelectron and soft X-ray emission spectra of water vapor.

3 Supplementary Tables

Samples	Solvent	Conc. (μM)	Time (min)	Temp. (°C)	M_n	$Đ$ (M_w/M_n)	σ (chains /nm^2)	Water contact angle (°)	Air contact angle (°)
Gold	-	-	-	-	-	-	-	81.6 ± 1.2	135.3 ± 0.4
gl-PMEA	methanol	1	20	RT	38,000	1.17	0.10	63.5 ± 1.4	140.9 ± 1.3
gc-PMEA	methanol	1	60	40	75,900	1.09	0.050	78.5 ± 1.8	142.5 ± 1.2

Table S1. Conditions used to prepare polymer grafts and the physical properties of the same.

Table S2. QCM analysis for hydrated gl-PMEA and gc-PMEA.

	Substrate number	$\Delta F_{grafted,air}$ (Hz)	$\Delta F_{grafted,water}$ (Hz)	σ (chains/nm^2)	$\Delta F_{grafted,water}/\Delta F_{grafted,air}$ (-)
gl-PMEA	No. 1	−114	−151	0.100	1.32
	No. 2	−116	−179	0.101	1.55
	No. 3	−119	−193	0.104	1.62
	Ave. ± SD	−116 ± 2	−174 ± 18	0.102 ± 0.002	1.50 ± 0.13
gc-PMEA	No. 1	−100	−149	0.044	1.49
	No. 2	−114	−181	0.050	1.58
	No. 3	−119	−193	0.052	1.62
	Ave. ± SD	−111 ± 8	−174 ± 19	0.049 ± 0.004	1.57 ± 0.05

For a method, please refer to section "Quartz Crystal Microbalance (QCM) Measurements" in this Supplementary Information. Abbreviations stand for the following:
gl-PMEA: linear-poly(2-methoxyethyl acrylate) grafted interface of gold-sputtered QCM substrates.
gc-PMEA: cyclic-poly(2-methoxyethyl acrylate) grafted interface of gold-sputtered QCM substrates.
$\Delta F_{grafted,air}$: frequency change between after grafting of PMEA and before measured in air (dry state).
$\Delta F_{grafted,water}$: frequency change between after grafting of PMEA and before measured in water.
σ: grafting density of PMEA.
$\Delta F_{grafted,water}/\Delta F_{grafted,air}$: ratio of apparent mass in the hydration state against the dry state.
Ave. ± SD: average with standard deviation.

1

Classification	Peak#1	Peak#2	Peak#3	Peak#3'	Peak#3"	Peak#4
Gas-like	Asym. Gauss X: 521.0 s: 1.0 Asym: 0.2(Fix)	Gaussian X: 525.5 s: 1.0 -	-	-	-	Lorentzian X: 527.1 g: 0.15
Isolate	Asym. Gauss X: 521.0 s: 1.0 Asym: 0.2(Fix)	Gaussian X: 524.0 s: 1.0 -	Gaussian X: 526.0 s: 0.9	-		Lorentzian X: 527.0 g: 0.10
Bulk-like	Gaussian X: 521.0 s: 1.0	Gaussian X: 524.5 s: 1.0(Fix)	-	Gaussian X: 525.5 s: 0.3	Gaussian X: 526.7 s: 0.3	-

2 **Table S3.** Fitting functions and initial parameters for X-ray emission spectra.

3

4 Reference

1. G. Sauerbrey, *Z. Physik.*, 1959, **155**, 206-222.